crystals

MDPI

Article

Effect of Polar Faces of SiC on the Epitaxial Growth of Graphene: Growth Mechanism and Its Implications for Structural and Electrical Properties

Stefan A. Pitsch [1,2] and R. Radhakrishnan Sumathi [1,*]

[1] Applied Crystallography and Materials Science Section, Department of Earth and Environmental Sciences, Ludwig-Maximilians-University (LMU), Theresienstrasse 41, D-80333 Munich, Germany
[2] Presently at Institute for Geochemistry and Petrology, ETH Zürich, Clausiusstrasse 25, 8092 Zürich, Switzerland
* Correspondence: sumathi@lrz.uni-muenchen.de

Abstract: In this study, epitaxial graphene layers of cm^2 sizes were grown on silicon carbide (SiC) substrates by high-temperature sublimation. The behavior of the two crystallographic SiC-polar faces and its effect on the growth mechanism of graphene layers and their properties were investigated. Crystallographic structural differences observed in AFM studies were shown to cause disparities in the electrical conductivity of the grown layers. On the silicon-polar (Si-polar) face of SiC, the graphene formation occurred in spike-like structures that originated orthogonally from atomic steps of the substrate and grew outwards in the form of 2D nucleation with a fairly good surface coverage over time. On the carbon-polar (C-polar) face, a hexagonal structure already formed at the beginning of the growth process. On both polar faces, the known process of step-bunching promoted the formation of nm-scale structural obstacles. Such a step-bunching effect was found to be more pronounced on the C-polar face. These 2D-obstacles account for a low probability of a complete nano-sheet formation, but favor 2D-structures, comparable to graphene nanoribbons. The resulting direction-dependent anisotropic behavior in electrical conductivity measured by four-point probe method mainly depends on the height and spacing between these structural-obstacles. The anisotropy becomes less prudent as and when more graphene layers are synthesized.

Keywords: 2D materials; graphene; silicon carbide; sublimation growth; surface morphologies; step-bunching; electrical conductivity

check for updates

Citation: Pitsch, S.A.; Sumathi, R.R. Effect of Polar Faces of SiC on the Epitaxial Growth of Graphene: Growth Mechanism and Its Implications for Structural and Electrical Properties. *Crystals* **2023**, *13*, 189. https://doi.org/10.3390/cryst13020189

Academic Editors: Justina Gaidukevic and Jurgis Barkauskas

Received: 13 December 2022
Revised: 15 January 2023
Accepted: 18 January 2023
Published: 21 January 2023

Copyright: © 2023 by the authors. Licensee MDPI, Basel, Switzerland. This article is an open access article distributed under the terms and conditions of the Creative Commons Attribution (CC BY) license (https://creativecommons.org/licenses/by/4.0/).

1. Introduction

Graphene has attracted much attention for its outstanding material properties such as strength, chemical durability, electrical conductivity and many more and is therefore extensively studied. Since its discovery in 2004, an exponential increase in the graphene material research could be observed. The reason is the material's high potential for multiple areas of application. Prominent examples are highly durable and strong mechanical components for the aviation and automobile industries, a new generation of solar cells, batteries and transistors, conductive inks, sensors [1], material for bio-medical applications [2], etc.

Graphene, ideally, is a single-layer material, solely composed of carbon atoms and arranged in a planar, hexagonal honeycomb lattice that accounts for many of its outstanding properties. Each carbon atom is bonded via sp^2 hybridized bonds to three other carbon atoms with a C-C distance of 1.42 Å [3]. Although graphene's properties largely depend on it being a single layer and free standing, i.e., chemically un-bound to other substrates, the term graphene is often used for bi-, tri-, and multilayers as well. As many as 10 layers have been reported to be graphene or to show graphene-like behavior [4].

The special bonding situation in graphene and its high lattice symmetry make it resistant to covalent modification and therefore chemically durable [4], highly efficient in

electron and heat transport and result in graphene to be the first zero bandgap semiconductor material that is known [5]. The electrical conductivity of intrinsic graphene is quite low in the order of the conductance quantum $\sigma \sim e^2/h$ because at the Dirac points, the density of states is zero. Via doping, either through an electric field or adsorption, the conductivity changes are to be quite high, even outperforming copper at room temperature [5]. Even strain in a graphene sheet, which has been shown never to be a completely flat surface [4], acts as a bandgap modifying parameter [5,6] and must be considered when measuring graphene's electrical properties.

Multiple ways of fabrication are known, with each individual one suffering from setbacks. Chemical vapor deposition is mostly stated when large-areas of graphene are grown with both high quality and uniformity, mostly on Cu/Ni and Si/SiO_2 substrates. Another formation mechanism is the formation out of SiC substrates. Extensive work has been carried out to fabricate good quality, large-area graphene [7–10] resulting in many different growth techniques that are being improved continuously. However, a well-controlled process which yields a defined (low) number of layers, even better, single crystals, remains a challenge [11,12]. Goals are a better control of surface morphologies, individual crystal sizes and homogeneity.

The epitaxial growth of graphene on silicon carbide (SiC), a process which is also known as the sublimation technique, relies on SiC as a substrate. Due to SiC's crystal structure, with a distance of the carbon plane to the neighboring Si plane having a ratio of 1:3 in relation to the C-C interplanar distance, two polar faces can be subclassified: The Si-polar face and the C-polar face [13]. For the case of the resulting Si-polar face ([0001]), Si atoms occupy the top positions, while in the case of the C-face ([000-1]), C atoms form the top respectively. Although there is a relatively high lattice mismatch of about 0.62 Å (3.073 Å for SiC versus 2.46 Å for graphene) between graphene and the used substrate, it has been shown that 6H-SiC (a specific polymorph of SiC) acts as a very good surface for the sublimation synthesis of graphene [1]. The growth process is driven by the preferred Si sublimation compared to its stoichiometric counterpart composing the substrate. For the growth of one layer of graphene at least 3 layers of SiC bilayers are necessary [14]. Decomposition of SiC starts preferentially where the binding energy within the substrate is lowest, which is mainly at defect sites and atomic terrace edges of the SiC substrate [15]. A detailed review of the growth process can be found in G. R. Yazdi [3].

Surface reconstructions and growth kinetics differ for each polar surface. This results in different graphene growth rates, morphologies, and electronic properties for the graphene on the two polar faces [3]. The Si-face of SiC has the advantage that growth of graphene occurs much more slowly than on its counterpart and is therefore a lot easier to control by the growth parameters such as temperature and time alone. However, the Si-face also has worse electrical properties in comparison with the C-face due to a buffer layer that is formed before graphene formation occurs [16]. Generally, graphene on the Si-face is produced as a multilayer stack. The layers within interact with each other as they do in graphite, accounting for more and more graphite-like behavior the thicker the stacks become [17]. The Si-face produces domains that are only about a third of the size of graphene domains that were grown on the C-face. Under an argon atmosphere, domains could typically reach sizes of about 50 µm [1].

The growth of graphene on the C-face is faster, a lot harder to control and does not produce a buffer layer. From the first produced graphene layer onwards, no strong interaction with the substrate occurs any longer which results from a relatively large distance to the substrate (3.2 Å) and the absence of covalent bonds to it. Multilayers, in contrast to the Si-face, show a large amount of rotational disorder. Every single graphene layer in a stack of many thus behaves like a monolayer of its own because of the very weak interaction between the layers [3]. Therefore, graphene that is grown on the C-face generally shows better electrical properties and is able to retain those for quite thick stacks [17]. The intrinsic mobility of Si-face graphene is about two orders of magnitude lower than optimally grown graphene on the C-face due to its graphite-like behavior [14]. C-face graphene

was measured to reach 10,000 to 30,000 $cm^2.V^{-1}$ s^{-1} under room temperature while Si-face graphene yielded 500 $cm^2.V^{-1}s^{-1}$ to 2000 cm^2. $V^{-1}s^{-1}$ at the same conditions [1]. Resistivity on SiC-grown graphene (grown on the [0001]-face) has been reported to be in the range of 1.2×10^{-4} Ω·cm to 7.4×10^{-5} Ω·cm [18].

Although the sublimation epitaxy, over time, received less attention than, for example, the predominant CVD growth method, sublimation growth of graphene is still a potential candidate for future use for its comparative ease in handling and investigating after the growth, compared with other techniques that require a transfer process off a substrate before consecutive processing. Special applications, among them the work on confined 2D materials, benefit from the sublimation method and an improvement of the thereby formed graphene (e.g., [19,20]). The problem in this technique, however, is the lack of control over the resulting physical attributes that result out of the formed graphene's size, quality and thickness and can be influenced by growth temperature, duration, substrate treatment and its crystallographic orientation, carbon supply, pressure in the growth chamber, heating rate, etc. [3,20]. An improvement on the control of these factors has been reported on 4H-SiC by face-to-face growth in ultra-high vacuum [21] and by polymer-assisted growth [20]. The crucial factor of the degree of substrate miscut in obtaining good and reproducible results was outlined in [22].

The main aim of this work is to contribute to the understanding of the growth mechanism on different polar faces of SiC substrates. One relevant process on the substrate's surface during the growth process is that due to different decomposition kinetics of structural units, atomic steps tend to combine in higher ones, which is called step bunching. This growth process does not yet allow for complete control in terms of both the number of layers that are produced and the morphology of the graphene sheet. In contrast to other methods that do allow for a control on those attributes such as CVD, this method's advantage lies in no need to further treat the produced graphene once it is prepared on semi-insulating SiC, which can remain pristine on the SiC substrate and will therefore not be damaged in necessary consecutive preparation procedures. Also, we report here for the first time, to the best of our knowledge, the interrelation in the characteristics of growth-related structural and electrical properties resulting from two different growth mechanisms on the two polar faces of SiC. It has already been reported, that the structure of graphene has big impacts on its properties [23] and that graphene which is formed on one of SiC's two polar faces varies greatly depending on the face it was grown on [3,24]. However, a difference in the growth morphology on the two polar faces has not been reported so far. The resulting growth-direction-dependent anisotropy of the electrical resistivity is investigated and discussed.

2. Materials and Methods

The graphene layers were grown on the 6H polytype of SiC (on-axis) which had semi-insulating behavior and thus allowed resistivity measurements of the graphitized surface on top without major influence of the substrate. SiC wafers were cut into small squares of 1 to 2 cm^2 and cleaned by immersing them subsequently in boiling isopropanol and acetone. The samples were put onto a graphite sample holder with the polar face of the substrate that was later to be investigated facing downwards. An excavation was adjustable there both in height and diameter to account for a local increase of Si vapor pressure to interact with the surface. The sublimation rate at the surface of the sample could thus be controlled. The samples were put into a furnace, which was heated under an argon atmosphere of 800 mbar, accounting for a retardation of the sublimation process which starts at approximately 1500 °C under an argon pressure in comparison to about 1150 °C under ultra-high vacuum [1]. To reach growth temperatures as high as 2070 °C, a certain routine (program) was kept throughout the experiments to account for constant conditions: After reaching 1000 °C under a high vacuum, argon flow was enabled, and the temperature was increased to 1400 °C. By reaching these starting conditions, a fast up-ramping of 40 °C/min was performed to the intended growth temperature, where it

was kept constant for the set duration of the experiment. The down-ramping of temperature mimicked the up-ramping process down to 1400 °C, where in theory, no Si sublimation from the substrate was taking place any longer [1]. The two principal parameters to be varied in these experiments were temperature and duration of growth. Argon-pressure in the sample chamber was kept constant. The growth temperatures were chosen between the high end of the spectrum of most cited studies (1900 °C) and 2070 °C both to extend the available spectrum of data and because models and personal observations have indicated that higher temperatures are favorable to grow larger, single-crystal graphene areas [25].

After the growth, the samples were analyzed by means of (1) Raman spectroscopy and (2) Atomic Force Microscopy (AFM) to be able to allow for an estimation of the numbers of graphene layers that were produced on the substrate and to observe the surface morphology of the samples. The (3) four-point probe measurement was conducted to be able to relate the observations to the electrical properties of formed material.

(1) Raman spectroscopy was used to qualitatively determine whether the growth of graphene on the SiC surface was successful. Graphene and graphite in Raman spectroscopy showed 3 major peaks that could be used to differentiate between both materials, namely the D, G and 2D peaks. In this study, the ratios of the 2D (2700 cm^{-1}) and the G peak (1582 cm^{-1}) were used for the differentiation. This ratio,

$$IR = I_{2D}/I_G, \quad (1)$$

where IR is the aforementioned intensity ratio, I_G is the intensity of the G peak, and I_2D is the intensity of the 2D peak, was used to identify single, free-standing graphene layers, which are indicated by an IR value of ~2. Ratios between 1 and 2 have been reported to show monolayer graphene, however, still attached to the substrate [26]. This ratio decreases with an increasing number of layers, eventually resulting in a ratio of about 0.25 for graphite. To evaluate the thickness of the graphene layers further, an additional intensity ratio (IS) is used, taking into account the Raman signal of the underlying SiC substrate (1518 cm^{-1}). This ratio is calculated as the following:

$$IS = I_{substrate}/I_G \quad (2)$$

As in Raman spectroscopy, only the topmost atomic layers contribute to most of the signal intensity, this ratio can be used to qualitatively quantify the thickness of the graphene stack on top of the substrate. If IS is high, the underlying substrate has a high influence in the measurement which points towards a thin layer of graphene coverage on the surface and vice versa.

The full width at half maximum (FWHM) of the 2D peak allows a distinction of mono- and multi-layered graphene, which is 24 cm^{-1} for a free-standing single layer of graphene. Double, triple and multi layers show significantly higher FWHMs [27] and non-free-standing monolayers have been reported to show a FWHM of around 40 cm^{-1} [26]. The 2D peak allows for additional information about strain on the graphene lattice, which derives from both a slight mismatch between the crystal lattices of graphene and SiC about 0.62 Å [1] and from having inversely behaving thermal expansion coefficients [28,29]. It has been shown that during cooling, compressive strain of up to 0.8% accumulates in the graphene sheets, which is measurable by a corresponding blue-shift in G and 2D bands of about 22 cm^{-1} [29]. Additional stress would result in even higher shifts of the peak positions.

The selected wavelength for the laser was 532 nm with 100% intensity reaching the sample. The error of the measured Raman shift that derives from the instrument is given as a maximum shift of 1.5 cm^{-1} into both directions. To evaluate the samples, both mappings with an area of 180 × 360 μm^2 (with 100 single, equally spaced measurement points) as well as the arbitrarily chosen single-point measurements were conducted. To allow a direct comparison of overall quality between the samples, an arbitrary space was mapped in

the middle of all the samples. The single-point measurements were used to search for the biggest area of the desired single layer-free-standing graphene.

(2) AFM was used to produce surface images of the samples and to determine topographic differences between graphene grown on the two polar faces of SiC. AFM was conducted in constant force mode. The typical step height of a single graphene layer was reported to be 0.275 ± 0.001 nm, but the friction and the effect of impurities and physisorbed water could affect the measured topography considerably [30]. The linear correction mode was used for the images, which is the reason why profile lines in the figures show terraces that make the impression that they are inclined.

(3) The four-point probe technique, which is a system of 2 separate current- and voltage-sensing electrodes, used to measure extremely low resistance values, was used to measure the electrical resistivity ρ of the samples. The spacing between the probes is 1 mm. For thin films, the equation

$$\rho = \Pi/\ln 2 \times t \times V/I \quad (3)$$

was used, with I being the applied electrical current, V the measured voltage and t the thickness of a conducting layer. From this formula, it is evident, that one has to know the thickness and thus the number of graphene layers that have been grown on the substrate. This was assumed to range between 2 and 10 layers for the samples of this study and was individually set to a value in this range from the observations from the other two measurement techniques. For all samples, 4 directions (two diagonal and 2 orthogonal) were conducted. Each directional value represents the mean of 10 individual measurements of the same orientation on the sample within ±0.5 mm at the same spot. Following this procedure, for all samples at least 6 individual values in all 4 directions were produced. The minimum value of each direction is reported as an average of all individual measurement cycles of different spots on the sample, evaluated at the same orientation. The highest values, which correspond to a measurement direction perpendicular to the lowest values are also reported.

3. Results

3.1. Raman Spectroscopy

As described in previous sections, the shape, position, and height of peaks can be used to determine few and single-layer graphene from Raman spectra [31]. A typical spectrum of a mapping (one hundred equally spaced point measurements) on a C-polar face of SiC from our experiments is depicted in Figure 1 with the theoretical isolated spectrum of a monolayer graphene. Table 1 summarizes most important information about the samples relevant for this study as well as the results obtained from Raman and AFM measurements. Differences in observed characteristics at similar growth conditions (StGr-3 and 7) may be explained by slight technical deviations from the on-axis cutting angle of the industrially produced SiC substrate, which has been shown to have large effects on the resulting growth kinetics and developing structure [22].

3.1.1. Si-Face

Generally, the Si-face produces graphene with an IS ratio of 2.5 or above, which indicates a strong influence of the SiC substrate and therefore points to a reasonably thin graphitized surface. It can thus be said that for all samples, graphene-like material was formed, not graphite. The coverage of the graphitized surface ranges from an estimated complete (100%) down to 53%. It can be noted that a complete coverage of the graphitized surface is not necessarily a positive thing as these samples often showed very thick stacks of graphene or even spots of graphite in some places, in extreme cases. The maximum area of monolayer graphene which was detected is approximately 30 × 40 μm^2. It must be noted, however, that these areas do not correspond to single-crystal graphene. Single-layer graphene, here, corresponds to an area, which was found to be formed predominantly by single layer graphene, with multi-layers or holes as possible smaller textural aberrations within the monolayer. The determined blue shift of the 2D peak of about 20 cm^{-1} indicates

that the graphene is strained in a compressive manner [29]. Generally, for all Si-faced samples it was assumed that few-layer graphene was grown over the largest part of the surface area. When comparing the characteristic shapes of the 2D peak, all shapes that were described in the literature [1] are present in all samples. However, 5 to 7-layer stacks (estimated from IR ratio and shape) seem to be most abundant. The repeating FWHM of the 2D peak of 50 to 60 cm^{-1} corresponds to multilayers and substrate-attached stacks as well [29].

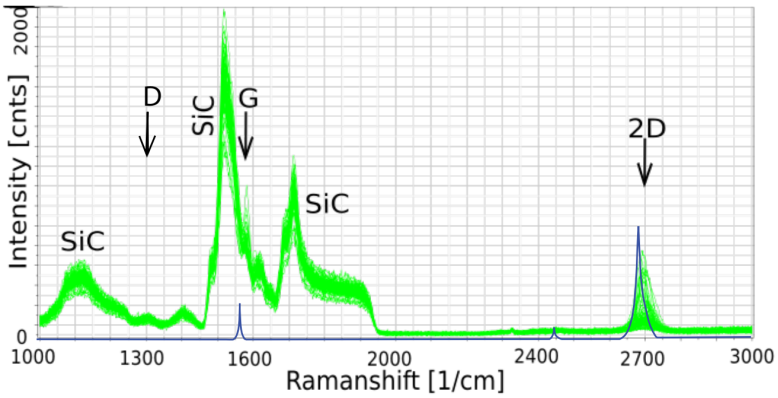


Figure 1. Measured Raman spectra of a characteristic sample with the signature of a 6H-SiC substrate (marked as SiC) with characteristic graphene peaks (marked as D, G and 2D). The green curves represent mapping spectra of 100 equally spaced points within the area of a typical Raman mapping (100×100 μm^2). Each individual spectrum corresponds to graphene grown on the C-polar face of SiC. For comparison, the typical spectrum of a monolayer graphene without a signature of a SiC substrate beneath the layer is plotted in blue as a reference. These reference data were replotted from [1].

3.1.2. C-Face

The C-face showed IS ratios between 2.5 and 3 for all samples, which indicates a thinner graphitization coverage compared with the Si-faced samples. The highest estimated percentage of monolayer coverage was found to be about 10% and the maximum detected area of monolayer graphene measured about 300×30 μm^2. Again, like Si-face, it must be noted here that these areas do not correspond to single-crystal graphene and single-layer graphene, but corresponds to an area, which might contain multi-layers or holes as possible smaller textural aberrations within the monolayer. Apart from sample StGr-3, all these samples showed a characteristic bulk FWHM of the 2D peak of around 45 cm^{-1} which is both characteristic of attached monolayers as well as few-layer graphene [26]. All the samples showed a small blue shift in the 2D peak, indicating compressive strain in the material probably resulting from reverse thermal expansion behavior of substrate and graphene.

3.1.3. Reproducibility

In order to determine the reproducibility of graphene grown on the same SiC-polar faces, more samples would have been needed to make detailed observations about the growth conditions and the effect of their change on formed graphene. The main objective of this work however, was finding the difference of the growth characteristics between different SiC-polar faces that can be seen and reproduced to a high degree. These are (1) Generally lower 2D peak widths on the C-polar face compared with the Si-polar face, (2) constant negative 2D peak shifts on the C-polar face, while the Si-polar face shows both negative and positive shifts, (3) larger, yet more irregular and elongated (eccentric) forms of single-layer areas grown on the C-polar face at the same growth conditions (time, duration), while Si-polar face grown graphene areas are less eccentric in nature, (4) Higher graphene surface coverages on the Si-face at the same growth conditions, (5) Higher observed step-heights on the C-polar face with larger ones forming at lower growth temperatures.

Table 1. List of all the samples, showing the information about the basic growth parameters as well as the most important results. The abbreviation ND means that there are no data available. For the samples where numbers are replaced by lines, there was either no signal detected or the condition 2D > G was untrue.

	Samples (Numbered w.r.t. Growth Experiments)									
Parameters	**StGr-1**	**StGr-2**	**StGr-3**	**StGr-4**	**StGr-5**	**StGr-6**	**StGr-7**	**StGr-8**	**AGr -12**	**AGr-13**
T of growth (°C)	2000	2000	2000	1900	1900	1900	2000	1900	2050	2070
duration of growth (s)	300	150	150	150	150	150	150	150	300	300
Heating rate after 1400 °C (°C/min)	40	40	40	40	40	40	40	40	40	40
Polar face graphene was grown on	Si	Si	C	C	C	Si	C	C	Si	Si
2D average peak width (cm^{-1})	50	60	65	45	40	70	40	-	60	60
average shift of 2D (cm^{-1})	−20	10	−15	−10	−10	20	−10	-	−10	0
2D average peak width where 2D/G > 1 (cm^{-1})	37	57	63	45	44	60	42	-	-	ND
shift of 2D where 2D/G > 1 (cm^{-1})	−10	−5	−5	−7	−8	−10	0	-	-	ND
maximum area of monolayer graphene found (μm^2)	30 × 40	30 × 30	30 × 40	90 × 60	80 × 60	20 × 40	300 × 30	0	0	0
coverage of graphene-like surface (%)	93	69	90	75	61	53	81	0	100	ND
IR ratio (average 2D/G) without substrate only points	0.33	0.25	0.33	0.41	0.23	0.18	0.42	0.16	0.33	ND
IS ratio (average substrate/G)	2.36	2.61	2.52	3.70	2.93	3.29	2.40	2.81	2.50	ND
Maximum step height (nm)	13	12	25	30	29	13	26	35	10	10
Hexagonal network	Yes	Yes	Yes	Yes	Yes	No	Yes	No	No	Yes
Interpretation (formation features) MM = Multi and monolayers	MM	MM	Thick graphene and graphite	MM	MM	Started, yet incom-plete growth	MM	Almost no graphene present	MM	MM

3.2. Atomic Force Microscopy

3.2.1. Si-Face

Generally, all Si-face grown samples that went through the sublimation process displayed similar surface features, only varying in how severe these features were developed depending on the temperature and the time of growth. The former smooth, polished surface of the substrate became much rougher. Bigger steps of up to 9.5 nm vertical displacement dominate the surface with large terraces in between them. Using lower magnifications, it could be seen that these steps form a superstructure with a certain repetitive order (Figure 2a). In-between higher steps (in the following described as bunched steps), smaller ones can be found in a sub-parallel order with vertical step heights of about 0.2 to 1.5 nm. The smaller steps often display spike-shaped fronts that are orthogonal to the step structure. The spikes were measured to have typical step heights of around 2.5 to 3.5 Å(Figure 2b,c). These spikes are interpreted as the growth front of a new graphene layer/film on the surface. The height of around 3 Årepresents the typical height of one monolayer graphene. Further, these spike shapes could optimally be related to a starting growth front of one new layer of graphene.

Often, the surface showed a sub-hexagonal network of bright lines that are slightly elevated relative to all other features (Figure 3a). These lines span the whole surface and run over both small steps and bunched steps alike. Typical heights of the lines relative to the structure beneath them were measured to range between 0.5 and 1.3 nm. In some instances, the hexagons are replaced by pentagons or heptagons, displaying the presence

of defects. Usually, networks of very pronounced hexagonal shapes showed a second, very faint network beneath them (Figure 3b). The bottom network is oriented like the more pronounced one, however is an independent structure. The maximum step-heights of the underlying network were determined to be typically between 1.5 and 3 Å(small peaks in Figure 3c) and are thus difficult to measure and may represent one layer of graphene.

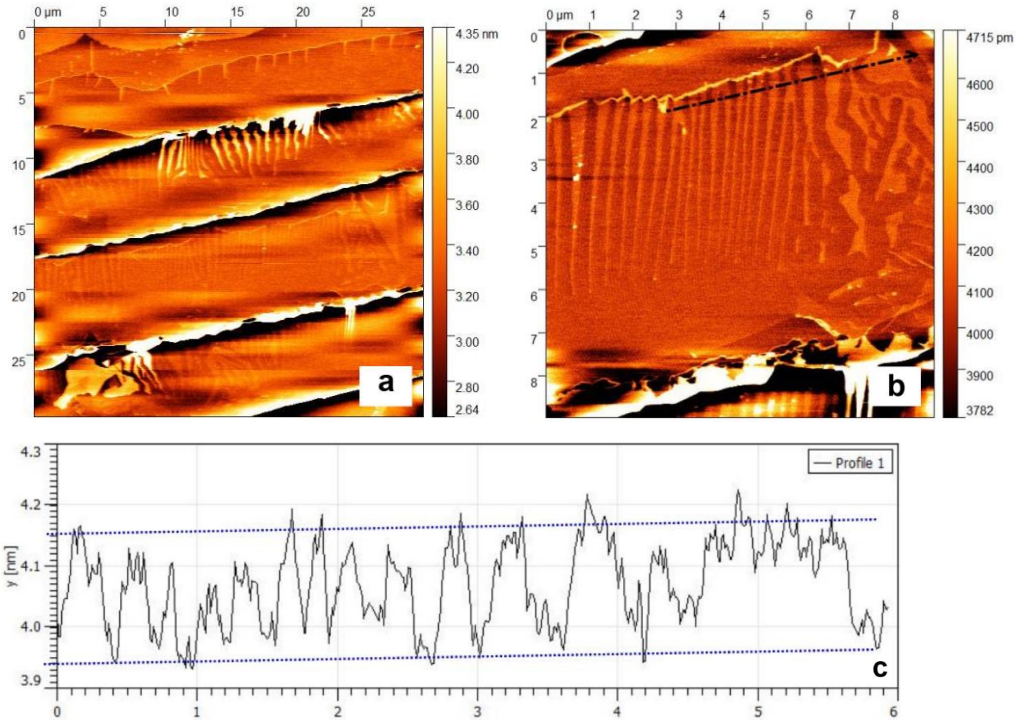


Figure 2. (**a**) 30 × 30 μm^2 of the graphitized surface of sample StGr-6. Bigger, parallel steps of about 4.5 nm in height are visible, running approximately from left to right in the picture. On the terraces between the steps, slightly brighter, slim fingers grow in the direction of the next step that is oriented higher than the point they originate from; (**b**) 9 × 9 μm^2 close-up of these bright fingers. The dashed black arrow indicates the trace of the height-profile depicted at the bottom (**c**); (**c**) 6 μm long profile across the surface of a terrace where a characteristic growth front of a sample grown on the Si-polar face of SiC. Dashed blue lines indicate the minimal height detected of the growth front; and the approximate mean of the valleys in between them respectively.

The elevated lines are seen as borderlines or overlapping regions of two adjacent hexagonal flakes of graphene—hence the elevation. Here it is interpreted that the elevated borderline of the lower graphene network deforms the topmost thin flakes growing above them. This causes the border zone to be traceable through the topmost layer. The stiff, yet bendable graphene on top smooths the surface expression. This is the reason why overlapping areas of individual flakes of the top layer (about 0.3 nm step height) are easily distinguished from the same structures one layer beneath (about half that height) that are not as pronounced and are cut by the bigger flake boundaries. The presence of an underlying structure directly confirms the Raman measurements, which predicted that predominantly multilayers were grown. Often, the surface displays small elevations that follow a random shape without interrupting it in a significant way. It is not trivial to differentiate between those and the crystal boundaries of the graphene, which are clearly hexagonally shaped and of smaller dimensions on the Si-faced substrate. The other elevations, however, often die out, branch out or show a zig-zag appearance. Even those can follow a pseudo hexagonal structure in some areas but have higher characteristic elevations. They can be interpreted as wrinkles, deformations of the surface that are usually formed during the cooling down process and are a direct effect of the different thermal

expansion coefficients between SiC and graphene. One example of these wrinkles can be seen in Figure 3a.

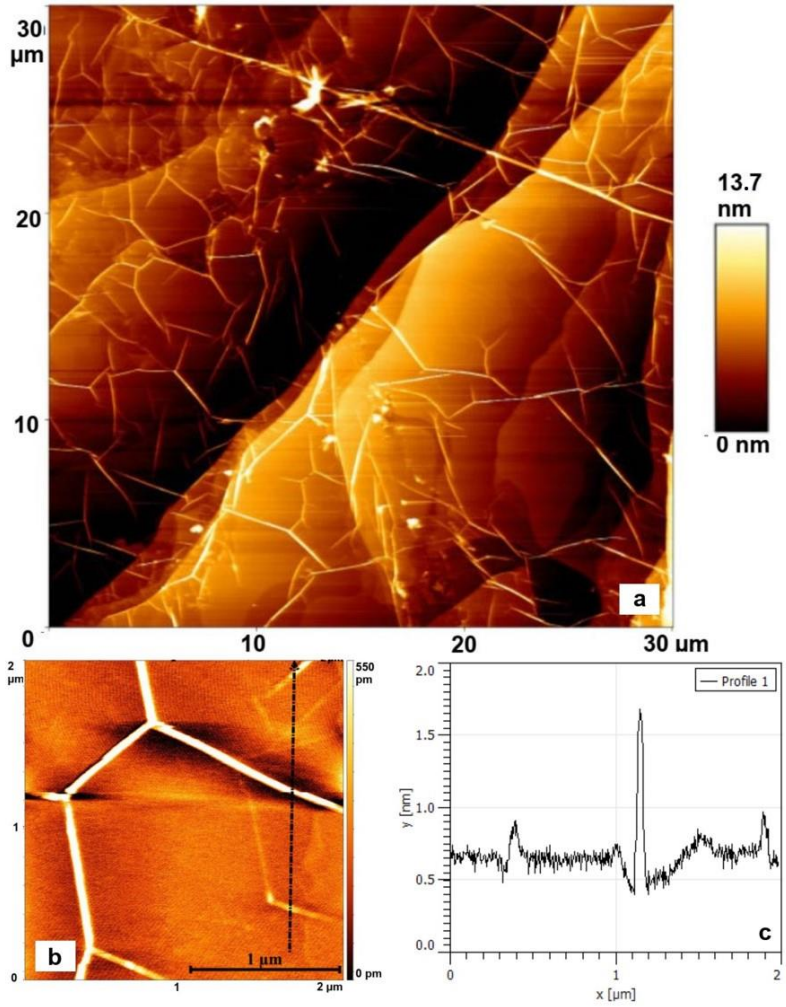


Figure 3. (**a**) 30 × 30 µm^2 of the graphitized surface of sample StGr-1. Visible are bigger steps of about 12 nm height where they coalesce, running diagonally from bottom left to top-right of the picture. On top of the surface, bright lines that create a pseudo hexagonal network. They are taken as wrinkles on the surface; (**b**) 2.1 × 2.1 µm^2 close-up of these bright lines. The dashed black arrow indicates the trace of the height-profile depicted on the right, (**c**); (**c**) 2 µm long profile across the surface. The trace of the profile-line can be viewed on the left (**b**).

3.2.2. C-Face

As in the case of the Si-polar face, the C-face displays a superstructure consisting of bunched steps. These bunched steps occur in a periodic arrangement, usually parallel to each other. Distances between them range from about 20 to 30 µm. This superstructure shows a medium-range structure on top of it, which is composed of steps as well. Medium-range steps (in the following m-steps) do not necessarily have to be parallel to each other and seem more randomly oriented compared to the bunched steps and may split up and reconnect again. The resulting are medium-range terrace islands that have shapes of lenses or stripes depending on the random orientation of the m-steps. Typically, one bunched step has five to seven m-steps in between. This accounts for step heights of roughly 3 to 4 nm and medium-range terrace widths of up to 9 µm. It is important to note that there is a variation in the distances of these m-steps to each other that does not seem random. The closer they are located to the lowest point of a terrace next to a bunched step, the closer the m-steps are situated to each other (Figure 4a–c). On smaller scale, a set of lines, like

those found on the Si-face can be found and are again considered as the representation of overlapping grain boundaries of graphene on the surface, as well as wrinkles of graphene on the 2D structure. Some very distinctive small-range features that were found to a varying degree on every sample were hexagonal fronts at small-range steps. Typically, they are composed of a mixture of halves of hexagons arranged together to produce an armchair-shaped growth front of individual graphene layers. The difference in height across such an armchair-shaped front was characteristically in the range of 3 Å (Figure 5a–c). The growth fronts are typically found where many small-range steps are concentrating in the vicinity of an m-step, from which the growth front originates. They exclusively start growing from the bottom of such an m-step which clearly shows the formation of a new layer of graphene.

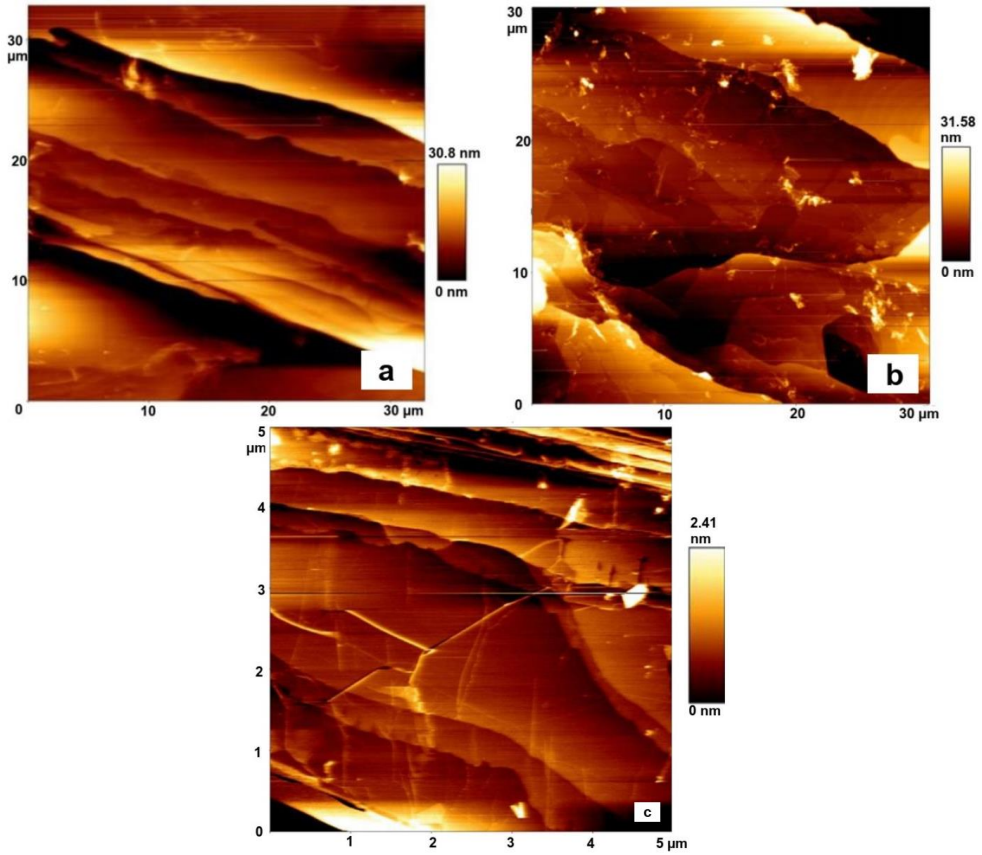


Figure 4. (**a**) Overview of the superstructure in the sample StGr-5. Bunched steps occur in periodic distances of about 15–20 µm to each other with step heights up to 20 nm. Smaller steps (medium range steps) do have approximately one fifth of both the step height and the distance compared to the superstructure. For yet smaller features, a higher magnification is necessary; (**b**) The same superstructure is visible in the other sample, StGr-7, but the medium range structure follows a more random order here. On top of the medium-range steps, small-range structures are faintly visible; (**c**) 5×5 µm^2 image showing a section of the graphitized surface of the sample StGr-5. Several steps can be seen with several growth fronts that all face towards the bottom-left of the picture. This structure is the fine-structure that can be found in between the bunched steps and m-steps which are displayed in (**a**,**b**). Over the visible terraces, two kinds of separations may be visible. The first is a distinctive set of lines, standing out about 1 nm from the mean height of the terrace. These lines often form 120° angles and cross small-range and medium-range steps in an undisturbed manner while being typically oriented at high angles to them. The second set of lines is less pronounced and never shows more than 0.6 nm difference in height to the surroundings. Typically, they are at very high angles close to 90° to small-range steps, where they often stop. These lines never cross medium-range steps.

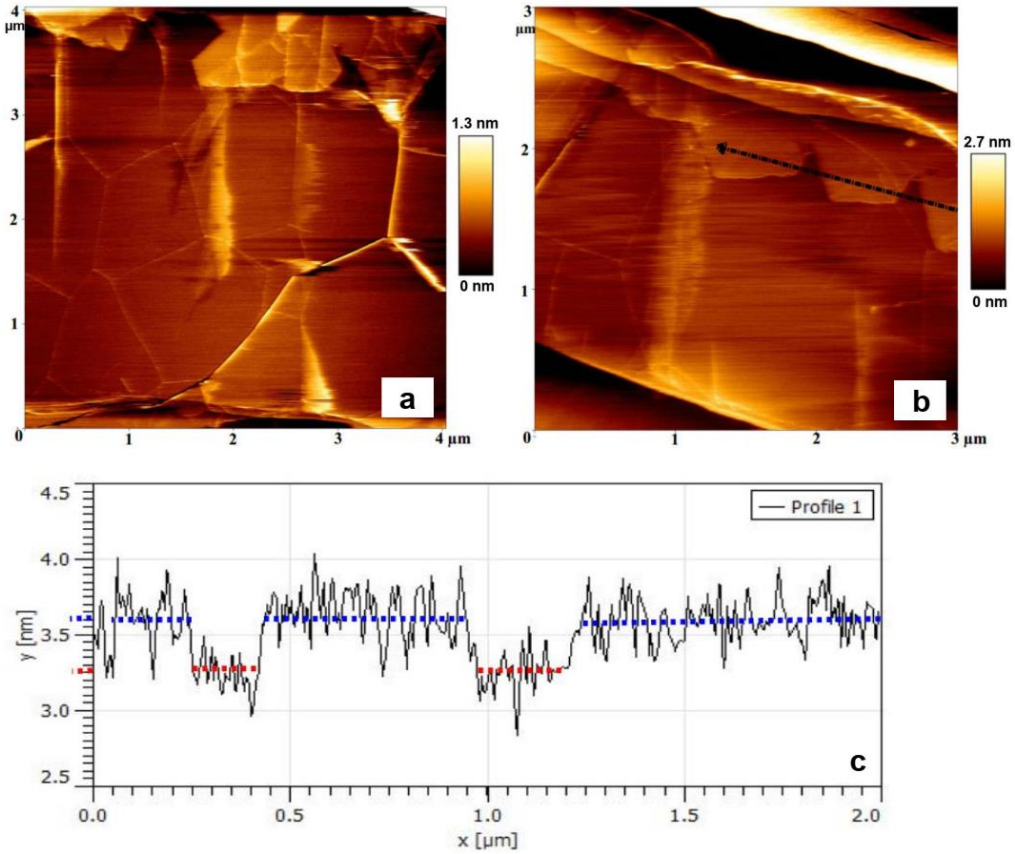


Figure 5. (**a**) Image of 4 × 4 µm^2 surface of the sample StGr-5 showing hexagonal structures. Both sets of lines that were described above, in Figure 4, are forming a hexagonal network over the surface of a terrace. Hexagons are replaced by pentagons or heptagons in some places as structural defects; (**b**) image of a 3 × 3 µm^2 area, both showing a hexagonal network as well as a growth front with a newly forming sub-hexagonal structure. The arrow indicates the trace of the profile-line that is shown below; (**c**) profile line taken over the boarder-zone of a newly forming hexagonal growth front of a sample grown on the C-polar face of SiC. The red and blue dashed lines indicate the average height of the terrace and the overgrowing growth-front.

4. Discussion

Because of different growth temperatures and growth durations, all observed features occurred to a varying degree in all samples. Exceptions to this observation (StGr 3 and 7) can be explained by a technical (slight) offset of the on-axis substrate which have a strong effect on the experimental result [22]. No two batches of wafers are completely identical. In consequence, a substrate that has slightly more atomic steps on its cut surface may produce a different result. As noted before, a general distinguishable trend between samples grown on Si and C-polar faces of SiC can be observed even though exact results cannot be reproduced between individual experiments that are grown on similar polar faces under the same growth conditions.

It was evident that samples which experienced the highest growth-temperature and duration also showed the highest amount of change in appearance as compared with the reference substrate. The spike morphologies on the Si-faced samples, with their terrace heights in the range of 3 Åcan be seen as the direct expression of a new graphene layer starting to form, as can be the half-hexagons on the C-face, respectively. Resulting from the described slower growth rate on the Si-polar face in the literature [3,16], one would expect the complete opposite growth geometry of a newly forming graphene surface. However, spike-shaped structures, as observed on the Si-polar face samples, are similar to skeletal or cellular growths in 3D crystal growth and thus have fast growth kinetics. An almost

idiomorphic growth of the graphene, indicated by the hexagonal growth front on the samples that were grown on the C-polar faces, is indeed more characteristic for higher equilibrium conditions and slower growth kinetics.

Both the polar faces of the substrate produce graphene surfaces, where the small-range hexagonal network (seen as the fingerprint of individual graphene flakes) does not grow over the bunched steps which are therefore seen as separation lines for the graphene growth. A sketch can be found in Figure 6. A uniform and unlimited 2D growth over the whole surface remains, therefore, a challenge. The result from this interpretation would be that bands of graphene form between separating bunched steps, forming a structure that can be close to graphene nanoribbons. The width between these bunched steps seems to pin down the area, where graphene growth can occur in an unhindered way. The m-steps and small range steps are therefore considered as individual growth fronts. Monolayers would thus be limited to the higher end of a bunched step and be a function of the distance between the bunched steps. How temperature and duration affect the distance of the bunched steps and their height is difficult to state from this data set, as the experiments did not cover a big range of temperatures and growth times because the goal was to improve the general quality of the graphene and to study the interrelation of surface structures and electrical conductivity. However, it is suggested that a higher growth temperature and a lower growth duration led to a lower degree of medium and small range structures and less order on the surface of the sample with a higher probability of interconnection between ribbons of graphene between bunched steps. The resulting surface would be best described as weakly interconnected nanoribbons. The fact that these ribbons are connected in places, however, can be seen when studying the wrinkle structures in the AFM images. They do not always end at a bunched step but may run over it, indicating that there has to be a connection surpassing a bunched step and thus a closed surface of graphene.

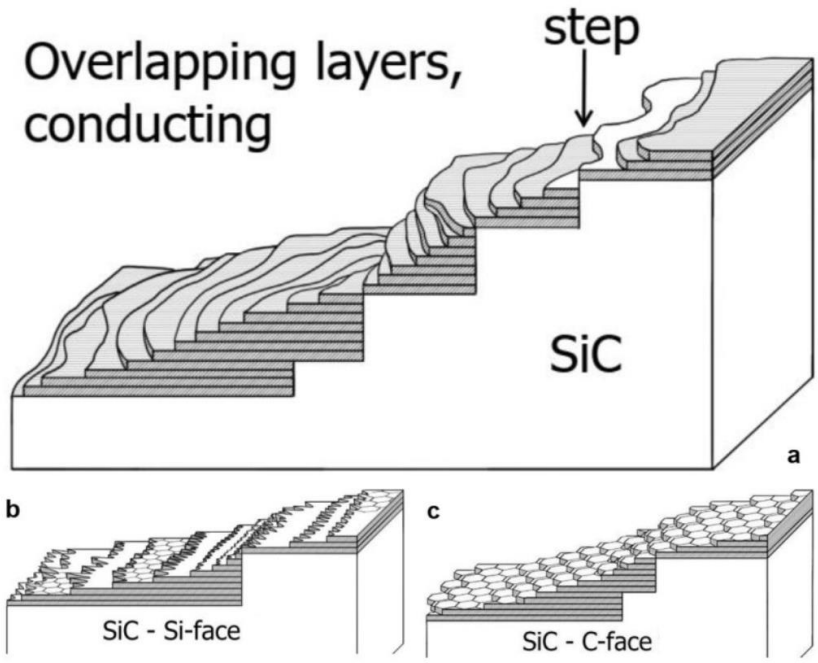


Figure 6. Schematic representation of the stock work of graphene layers on a SiC substrate. (**a**): An over-representation of atomic steps on the depicted substrate to be able to demonstrate the structure better. The substrate was an on-axis, industrially cut SiC wafer. Thus, some atomic steps could not be avoided, even though technically the substrate was cut in crystallographic plane orientation. Overlapping graphene layers allow for step-normal conductivity, while steps that are not completely overgrown account for a limited conductivity; (**b**,**c**): schematic figure, showing the difference in growth geometry of graphene on the two polar faces of SiC.

4.1. Four-Point Probe Measurements

The first important feature to notice for all the samples was that the electrical properties depend strongly on the direction of the measurement. Macroscopically, the layers look very uniform on the SiC surface, and hence their global electrical resistivity was measured using the four-point-probe technique. In each measurement, nearly a 3 mm area was measured, and the resistivity was calculated using Equation (3). Some samples showed directional differences in their electrical resistivity that could reach up to one order of magnitude. The reason for this will be subject to discussion in the section below. The resistivity values for graphene sheets of two, five and ten layers (these thickness values were being assumed based on various measurements) were calculated for each individual sample. Based on the observations depicted in Table 1 (IR, IS, width of 2D), the most likely average layer-thickness was chosen (indicated in green in Table 2).

Table 2. Results of the resistivity measurements for all samples. The values indicate the average of several measurements at different spots at the same orientation, using Equation (3) for an assumed graphene sheet of 2 layers (6.7 Å), 5 layers (16.75 Å) and 10 layers (33.5 Å). The samples StGr-1, StGr-2, StGr-6, Agr-12, Agr-13 were grown on Si-face. The other samples were grown on the C-face of SiC. Sample StGr-8 did not show a complete cover of graphene on the substrate and thus did not produce any reliable results. Numbers colored in green were the ones that were found to represent the whole samples' graphene thickness best, resulting from all collected data.

Samples	**p [Ω.cm] as an Average of All Values in the Direction of the Lowest Values**			**p [Ω.cm] as an Average of All Values in the Direction of the Highest Values (Perpendicular to the Lowest Values)**	**SiC-polar Face**
	Assumed 2 Layers	**Assumed 5 Layers**	**Assumed 10 Layers**		
StGr-1	4.60×10^{-7}	1.15×10^{-6}	2.30×10^{-6}	1.01×10^{-6}	Si
StGr-2	1.30×10^{-7}	3.24×10^{-7}	6.49×10^{-7}	2.82×10^{-7}	Si
StGr-3	8.37×10^{-7}	2.09×10^{-6}	4.19×10^{-6}	2.98×10^{-6}	C
StGr-4	2.56×10^{-8}	5.20×10^{-7}	1.04×10^{-6}	6.29×10^{-7}	C
StGr-5	3.43×10^{-8}	3.89×10^{-7}	7.79×10^{-7}	3.26×10^{-7}	C
StGr-6	3.56×10^{-7}	4.90×10^{-7}	1.78×10^{-6}	1.58×10^{-6}	Si
StGr-7	1.54×10^{-6}	3.84×10^{-6}	7.68×10^{-6}	3.09×10^{-6}	C
StGr-8	-	-	-	-	C
AGr-12	6.61×10^{-7}	1.65×10^{-6}	3.31×10^{-6}	1.47×10^{-5}	Si
AGr-13	4.49×10^{-7}	2.25×10^{-6}	4.49×10^{-6}	1.79×10^{-5}	Si

The resistivity values are ranged around 10^{-6} to 10^{-8} Ω.cm independent of the polarity of the substrate. This range occurs in the vicinity of the theoretical value of pristine graphene, which was computed to be around 1.04×10^{-6} Ω.cm [6]. Graphene that is bent, strained or has other structural modifications, which is assumed for graphene grown by the sublimation method, should show even higher resistivity values [32], but this was not the case for all the samples in this study. The strain in the graphene which was already observed in Raman measurements and by wrinkles in the AFM is related to thermal expansion differences between the substrate and the graphene layer on top as well as to the adaptation of the graphene to roughness of the substrate which can either be a relict or derived from the growth itself. The lowest values of strain were achieved for samples (StGr-2, 4, 5, 7 and AGr 12 and 13), indicated by the lowest measured 2D peak shift. StGr 2, 4 and 5, where this observation coincides with a relatively well established continuous few-layer graphene coverage, showed the lowest measured electrical resistivity values by far with the addition of StGr 1. Samples StGr 7 and AGr 12 and 13 showed quite thick graphene stacks in a few places (StGr 7) or developed thick graphitized surfaces

that could almost be described as graphite, which is the reason why these samples have a higher resistivity (ca. 1 order of magnitude) compared with samples StGr 1,2, 4 and 5. Samples such as StGr-8 and 3 showed the highest resistivity values by far, which is easily explained because these samples had relatively low graphitization coverages compared with the others. Generally, there is no obvious difference between the values for the Si- and the C-face grown graphene. Samples that were regarded as best from the Raman and AFM investigation methods (e.g., sample StGr-1, 2, 4, 5) also displayed the lowest electrical resistivity values compared with the others.

The values that are calculated are subject to the interpretation of how many layers of actual graphene were grown. Additionally, structural differences such as homogeneity and graphene coverage in percent play a huge role. Most of the samples showed characteristic monolayer Raman peaks in some places, and yet non-graphitized spaces in others. Therefore, the thickness of these graphene sheets comes close to the ideal monolayer. However, as an average coverage of layers, it is assumed to lie most probably between 2 and 5 layers. For few samples (StGr-1, 2, 4, 5 and 7), a thickness of 2 layers is assumed, because all these samples comparatively often showed a strong substrate fingerprint in Raman and in the AFM measurements. The other samples are interpreted to have a graphene cover of at least 5 or 10 layers. This is assumed because of the high occurrence of graphite-typical peaks in the Raman measurements, as well as the thick and scaly appearance they showed in the AFM images.

Interpreted Results of Layer Thickness and Directional Dependence

By a closer examination, it becomes striking that most of the samples had a directional dependence (growth/step direction) on the determined electrical resistivity values. It ranged between a factor of 2 and about one order of magnitude between the samples. This observation is examined in detail by marking the orientation of the striations on the samples and noting the directional difference to the aforementioned parallel and diagonal four-point probe measurements. It was found that the highest resistivity always coincides to a direction being as close to perpendicular to the striations as possible. A sketch of this directional dependence can be seen in Figure 7. The striations were found to coincide with the direction and spacing of the bunched steps that were described in the AFM section. It is safe to assume that bunched steps act as obstacle for the electrical current to flow in the cases of all samples prepared in this study. This may be due to a high strain in the graphene lattice that produces a high scattering potential for electrons along the bunched steps, consequentially lowering conductivity (i.e., increased resistivity). Additionally, as was observed in the AFM images (Figure 3a), graphene films do usually not overgrow these bunched steps immediately so that the current may be limited to some specific spots at a bunched step where the step height is either low enough for graphene to grow over it or the stacking has become thick enough so that two graphene sheets on terraces can combine, as indicated by the wrinkles in the AFM images in some places.

Following this interpretation, the difference in growth of graphene on C versus Si polar face is considered important: As the C-face produced generally thicker stacks of graphene, the likelihood of a combination of two sheets over a bunched step seems higher on that polar face. Additionally, bunched steps on the C-face were approximately two or three times as high as on the Si-face. However, bunched steps had a higher tendency to split into two individual ones too. These split bunched steps rejoined to form a big step in other places again, which, created interspersed islands of possible connectivity. This favors the connection of graphene stacks over a bunched step on the C face too and might indicate that C-face sublimated graphene would be better in its electrical properties than the Si-face-grown graphene.

AFM images also showed that graphene crystals were generally smaller when the graphene was grown on the Si-face, which was also found by B. K. Daas [33]. This corresponds to a higher scattering of electrons on grain boundaries and a therefore lower net-conductivity which is the reason why the Si-face is not superior to the C-face as both

effects affect each other in a reciprocal manner. For the case of the high-temperature-grown samples (AGr-12 and 13), it is assumed that the graphene stack became thick enough so that bunched steps no longer posed an obstacle. They were simply overgrown. Both samples were produced with a much higher growth temperature and a higher growth-duration accounting for the formation of thick graphene stacks that were confirmed by Raman measurements. This may rule out the effect of bunched steps acting as obstacles for current flow on these two samples completely. However, AGr-12 and 13 are still subject to the effect of scattering on grain boundaries. As stated, growth of graphene on the Si-face happens with the formation of small spikes that start growing from the vicinity of a bunched step (perpendicular to it) while the C-face produces crystals that are less anisotropic in shape. The long axis of the spikes of the Si face thus creates more crystal boundaries in a direction parallel to the bunched steps compared with perpendicular to it and thus produce more scattering in that direction compared with the C-face, where hexagonal, isotropic growth was observed. According to literature [1], C-face graphene should demonstrate better electrical properties. Observed resistivity values are expected to be significantly lower than those measured on the Si-face grown graphene. This was observed in our study as well. However, it also needs to be said that by taking the results of other measurement techniques into account, i.e., AFM, it was found that especially the C-face of the graphene showed big spots, where no growth had occurred.

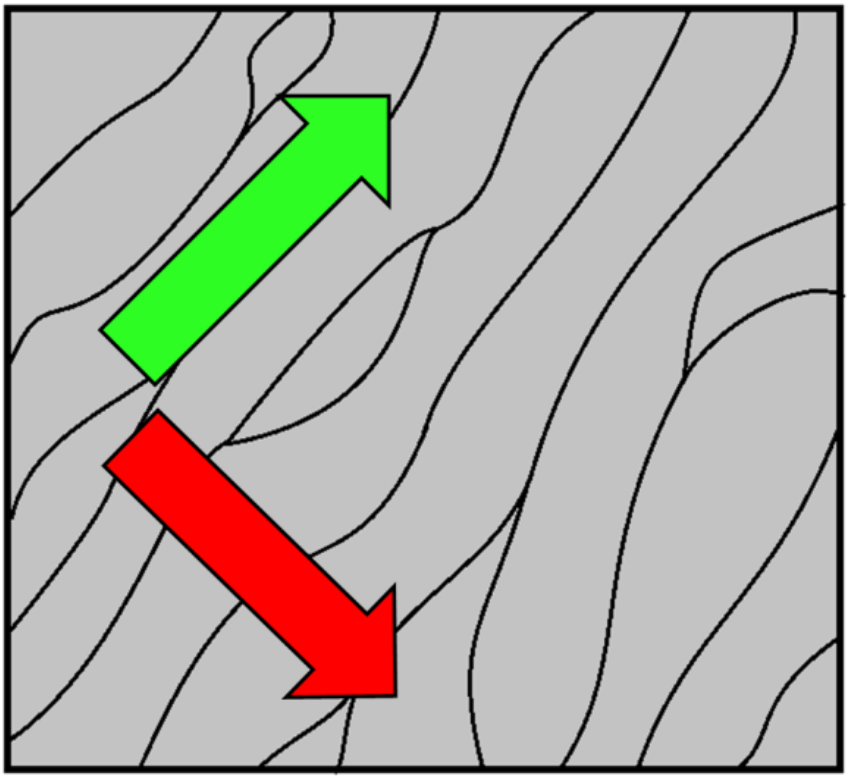


Figure 7. Schematic illustration of the directional dependence of the electrical resistivity on the structure of the layer. The box indicates a sample with steps and bunched steps that are indicated by the black lines. The green arrow indicates the direction that was found to yield lowest electrical resistivity (i.e., higher conductivity) values for thin graphene films. The red arrow indicates the direction of the highest resistivity values found on those samples. For thick graphene and graphite films, the directions are completely opposite.

5. Conclusions

The sublimation growth of epitaxial graphene on SiC was found to yield a few-layer graphene in most parts of the substrate up to 90% coverage. The substrate surfaces are covered by large-area flakes. The samples have at least one form of anisotropy in their

morphology, which could be connected to direction-dependent behavior in the conductivity measurements. Differences in electrical resistivity range from 2-times up to one order of magnitude. The lowest resistivity values were found for those samples that showed the highest degree of monolayer coverage combined with the highest amount of graphene coverage on its surface. These resistivity values were in the range of 2×10^{-8} Ω.cm. Directly measured sheet resistance values using the described 4-point probe technique ranged around 5 to 10 Ω.

Contradictory to the literature, which usually describes the preparation of epitaxial graphene on the C-face being hard to control, we obtained the best results on this face. This may be due to the difference in growth mechanism of the forming graphene layers, as depicted in Figure 6b,c, under the investigated and optimized growth conditions. However, occurrence of bunched steps of more than 10 nm height as a form of structural defect was observed from the growth process. The combined observations of AFM, optical microscopy and resistivity measurements indicate that these bunched steps also act as a barrier for the charge flow. In extreme cases, this may even result in a cluster of sub-parallel nanoribbons-like structures that are separated from each other. This is valid for the both polar faces, but the Si-face characteristically produces lower step heights. Bunched steps that form on the SiC substrate during the sublimation phase can indirectly be influenced, in terms of height and of distance to each other, via the main growth parameters such as temperature and time. The samples that had bunched steps in the periodicity of about 30 μm were found to display the best combination of properties for a later application. Still, the growth temperatures and growth durations that ranged between 1900 and 2000 °C would have to be optimized further to produce the highest surface coverage while maintaining thin graphene sheets and a good bunched step periodicity. The ramping time to achieve this high growth temperature may act as a limiting factor, since a relatively fast ramping would be needed to prevent extreme graphene formation already happening during the ramp-up period.

Any structural defects such as step bunches or clusters will deteriorate the device performance, and anisotropy in any properties such as conductivity is also not beneficial from device perspective. Further detailed investigation on the reduction of defects and anisotropy removal is currently underway, including simulation studies and the results will be reported. Even though the formation of anisotropic bunched terraces in combination with the growth mechanism of graphene on SiC substrate is not particularly ideal for closed isotropic sheet formation, it may offer a novel possibility to obtain separated nanoribbon-like structures on SiC substrates. With more controllability and a clear separation between the steps, this observation may lead to new possible application of that method for devices that rely more on nanoribbons than on isotropic sheets of graphene.

Author Contributions: Conceptualization, R.R.S.; methodology, S.A.P. and R.R.S.; formal analysis, S.A.P.; investigation, S.A.P. and R.R.S.; resources, R.R.S.; data curation, S.A.P.; writing—original draft preparation, S.A.P.; writing—review and editing, R.R.S.; visualization, S.A.P.; supervision, R.R.S.; project administration, R.R.S.; funding acquisition, R.R.S. All authors have read and agreed to the published version of the manuscript.

Funding: The financial support given by the Bavarian Equal Opportunity Promotion (Bayerische Gleichstellungsförderung, BGF) is gratefully acknowledged.

Data Availability Statement: Not applicable.

Acknowledgments: The authors are very grateful to P. Gille for all his encouragements during this work and Guntram Jordan for his help in doing AFM measurements. This article is part of Stefan A. Pitsch's master thesis work.

Conflicts of Interest: The authors declare that they have no known competing financial interests or personal relationships that could have appeared to influence the work reported in this paper.

References

1. Ferrari, A.C.; Bonaccorso, F.; Fal'Ko, V.; Novoselov, K.S.; Roche, S.; Bøggild, P.; Borini, S.; Koppens, F.H.L.; Palermo, V.; Pugno, N.; et al. Science and technology roadmap for graphene, related two-dimensional crystals, and hybrid systems. *Nanoscale* **2015**, *7*, 4598–4810. [CrossRef]
2. Lebedev, A.; Davydov, S.; Eliseyev, I.; Roenkov, A.; Avdeev, O.; Lebedev, S.; Makarov, Y.; Puzyk, M.; Klotchenko, S.; Usikov, A. Graphene on SiC Substrate as Biosensor: Theoretical Background, Preparation, and Characterization. *Materials* **2021**, *14*, 590. [CrossRef] [PubMed]
3. Yazdi, G.R.; Iakimov, T.; Yakimova, R. Epitaxial Graphene on SiC: A Review of Growth and Characterization. *Crystals* **2016**, *6*, 53. [CrossRef]
4. Geim, A.K. Graphene: Status and Prospects. *Science* **2009**, *324*, 1530–1534. [CrossRef] [PubMed]
5. Neto, A.C.; Guinea, F.; Peres, N.M.; Novoselov, K.S.; Geim, A.K. The electronic properties of graphene. *Reviews of modern physics* **2009**, *81*, 109. [CrossRef]
6. Novoselov, S. *Scientific Background on the Nobel Prize in Physics: Graphene*; The Royal Swedish Academy of Sciences: Stockholm, Sweden, 2010.
7. Cao, X.; Qi, D.; Yin, S.; Bu, J.; Li, F.; Goh, C.F.; Zhang, S.; Chen, X. Ambient Fabrication of Large-Area Graphene Films via a Synchronous Reduction and Assembly Strategy. *Adv. Mater.* **2013**, *25*, 2957–2962. [CrossRef]
8. Virojanadara, C.; Syväjarvi, M.; Yakimova, R.; Johansson, L.; Zakharov, A.; Balasubramanian, T. Homogeneous large-area graphene layer growth on 6 H-SiC (0001). *Phys. Rev. B* **2008**, *78*, 245403. [CrossRef]
9. Chen, X.; Zhang, L.; Chen, S. Large area CVD growth of graphene. *Synth. Met.* **2015**, *210*, 95–108. [CrossRef]
10. Li, X.; Cai, W.; An, J.; Kim, S.; Nah, J.; Yang, D.; Piner, R.; Velamakanni, A.; Jung, I.; Tutuc, E.; et al. Large-Area Synthesis of High-Quality and Uniform Graphene Films on Copper Foils. *Science* **2009**, *324*, 1312–1314. [CrossRef]
11. Huang, M.; Ruoff, R.S. Growth of Single-Layer and Multilayer Graphene on Cu/Ni Alloy Substrates. *Acc. Chem. Res.* **2020**, *53*, 800–811. [CrossRef] [PubMed]
12. Longo, R.C.; Ueda, H.; Cho, K.; Ranjan, A.; Ventzek, P.L.G. Mechanisms for Graphene Growth on SiO_2 Using Plasma-Enhanced Chemical Vapor Deposition: A Density Functional Theory Study. *ACS Appl. Mater. Interfaces* **2022**, *14*, 9492–9503. [CrossRef] [PubMed]
13. Izhevskyi, V.; Genova, L.; Bressiani, J.; Bressiani, A. silicon carbide. Structure, properties and processing. *Cerâmica* **2000**, *46*, 4–13. [CrossRef]
14. van den Berg, J.J. Spintronics and Thermoelectrics in Exfoliated and Epitaxial Graphene: Rijksuniversiteit Groningen. Ph.D. Thesis, University of Groningen, Groningen, The Netherlands, 2016.
15. Norimatsu, W.; Kusunoki, M. Formation process of graphene on SiC (0 0 0 1). *Phys. E* **2010**, *42*, 691–694. [CrossRef]
16. Kim, M.; Hwang, J.; Shields, V.B.; Tiwari, S.; Spencer, M.G.; Lee, J.-W. SiC surface orientation and Si loss rate effects on epitaxial graphene. *Nanoscale Res. Lett.* **2012**, *7*, 186. [CrossRef]
17. De Heer, W.A.; Berger, C.; Ruan, M.; Sprinkle, M.; Li, X.; Hu, Y.; Baiqian, Z.; Hankinson, J.; Conrad, E. Large area and structured epitaxial graphene produced by confinement controlled sublimation of silicon carbide. *Proc. Natl. Acad. Sci. USA* **2011**, *108*, 16900–16905. [CrossRef]
18. Kobayashi, K.; Tanabe, S.; Tao, T.; Okumura, T.; Nakashima, T.; Aritsuki, T.; O, R.-S.; Nagase, M. Resistivity anisotropy measured using four probes in epitaxial graphene on silicon carbide. *Appl. Phys. Express* **2015**, *8*, 36602. [CrossRef]
19. Kakanakova-Georgieva, A.; Ivanov, I.G.; Suwannaharn, N.; Hsu, C.-W.; Cora, I.; Pécz, B.; Giannazzo, F.; Sangiovanni, D.G.; Gueorguiev, G.K. MOCVD of AlN on epitaxial graphene at extreme temperatures. *Crystengcomm* **2020**, *23*, 385–390. [CrossRef]
20. Chatterjee, A.; Kruskopf, M.; Wundrack, S.; Hinze, P.; Pierz, K.; Stosch, R.; Scherer, H. Impact of Polymer-Assisted Epitaxial Graphene Growth on Various Types of SiC Substrates. *ACS Appl. Electron. Mater.* **2022**, *4*, 5317–5325. [CrossRef]
21. Zebardastan, N.; Bradford, J.; Lipton-Duffin, J.; MacLeod, J.; Ostrikov, K.K.; Tomellini, M.; Tomellini, M.; Motta, N. High quality epitaxial graphene on 4H-SiC by face-to-face growth in ultra-high vacuum. *Nanotechnology* **2022**, *34*, 105601. [CrossRef]
22. Yakimova, R.; Virojanadara, C.; Gogova, D.; Syväjärvi, M.; Siche, D.; Larsson, K.; Johansson, L.I. Analysis of the Formation Conditions for Large Area Epitaxial Graphene on SiC Substrates. *Mater. Sci. Forum* **2010**, *645–648*, 565–568. [CrossRef]
23. Lee, J.-K.; Yamazaki, S.; Yun, H.; Park, J.; Kennedy, G.P.; Kim, G.-T.; Pietzsch, O.; Wiesendanger, R.; Lee, S.; Hong, S.; et al. Modification of Electrical Properties of Graphene by Substrate-Induced Nanomodulation. *Nano Lett.* **2013**, *13*, 3494–3500. [CrossRef] [PubMed]
24. Srivastava, N.; He, G.; Luxmi; Mende, P.C.; Feenstra, R.; Sun, Y. Graphene formed on SiC under various environments: Comparison of Si-face and C-face. *J. Phys. D Appl. Phys.* **2012**, *45*, 154001. [CrossRef]
25. Zhang, W.; Van Duin, A.C.T. Atomistic-Scale Simulations of the Graphene Growth on a Silicon Carbide Substrate Using Thermal Decomposition and Chemical Vapor Deposition. *Chem. Mater.* **2020**, *32*, 8306–8317. [CrossRef]
26. Bao, J.; Yasui, O.; Norimatsu, W.; Matsuda, K.; Kusunoki, M. Sequential control of step-bunching during graphene growth on SiC (0001). *Appl. Phys. Lett.* **2016**, *109*, 81602. [CrossRef]
27. Malard, L.M.; Pimenta, M.A.; Dresselhaus, G.; Dresselhaus, M.S. Raman spectroscopy in graphene. *Phys. Rep.* **2009**, *473*, 51–87. [CrossRef]
28. Pierson, H.O. *Handbook of Carbon, Graphite, Diamonds and Fullerenes: Processing, Properties and Applications*; William Andrew: Noyes, NJ, USA, 1994.

29. Ferralis, N.; Maboudian, R.; Carraro, C. Evidence of structural strain in epitaxial graphene layers on 6H-SiC (0001). *Phys. Rev. Lett.* **2008**, *101*, 156801. [CrossRef]
30. Musumeci, C. Advanced Scanning Probe Microscopy of Graphene and Other 2D Materials. *Crystals* **2017**, *7*, 216. [CrossRef]
31. Ferrari, A.C.; Meyer, J.C.; Scardaci, V.; Casiraghi, C.; Lazzeri, M.; Mauri, F.; Piscanec, S.; Jiang, D.; Novoselov, K.S.; Roth, S.; et al. Raman spectrum of graphene and graphene layers. *Phys. Rev. Lett.* **2006**, *97*, 187401. [CrossRef]
32. Wojtaszek, M. Graphene: A Two Type Charge Carrier System. Master's Thesis, Faculty of Mathematics and Natural Sciences, Groningen, The Netherlands, 2009.
33. Daas, B.; Omar, S.U.; Shetu, S.; Daniels, K.M.; Ma, S.; Sudarshan, T.; Chandrashekhar, M.V.S. Comparison of epitaxial graphene growth on polar and nonpolar 6H-SiC faces: On the growth of multilayer films. *Cryst. Growth Des.* **2012**, *12*, 3379–3387. [CrossRef]

Disclaimer/Publisher's Note: The statements, opinions and data contained in all publications are solely those of the individual author(s) and contributor(s) and not of MDPI and/or the editor(s). MDPI and/or the editor(s) disclaim responsibility for any injury to people or property resulting from any ideas, methods, instructions or products referred to in the content.